Cellular and Molecular Biology
E-ISSN : 1165-158X / P-ISSN : 0145-5680
www.cellmolbiol.org

Nobiletin regulates invasion, migration and metastasis in hypopharyngeal squamous cell carcinoma

Marisol Rosas-Martínez, José Antonio González Rosales, Gloria Gutiérrez-Venegas*

Biochemistry Laboratory of the Division of Graduate Studies and Research, Faculty of Dentistry, National Autonomous University of Mexico, Mexico City 04510, Mexico

ARTICLE INFO

Original paper

Article history:
Received: May 18, 2022
Accepted: June 06, 2023
Published: July 31, 2023

Keywords:

Apoptosis, flavonoids, oral cancer

ABSTRACT

Head and neck squamous cell carcinoma carries a poor prognosis. Patients typically present with advanced disease and exhibit severe malnutrition at the time of diagnosis. Nobiletin (NOB) (5,6,7,8,3',4'-Hexamethoxyflavone) is a polymethoxyflavone that inhibits the proliferation and migration of various cancer cell types. To the best of our knowledge, its effects on hypopharyngeal squamous cell carcinoma have not been evaluated previously. This study examined the effects of NOB on the proliferation, migration, and invasiveness of the FaDu cell line derived from hypopharyngeal squamous cell carcinoma. We determined protein kinase phosphorylation by western blot analysis, migration by Transwell assay, and metastatic potential by enzyme-linked immunosorbent assay of vascular endothelial growth factor. NOB inhibited cell proliferation by 40% at concentrations of 15 µM and 40 µM and reduced migration and induced apoptosis at 50 µM by downregulating extracellular signal-regulated kinase, protein kinase B, and phosphoinositide 3-kinase. Our results suggest that the effects of NOB on FaDu cells are associated with protein kinase inhibition.

Doi: http://dx.doi.org/10.14715/cmb/2023.69.7.1 Copyright: © 2023 by the C.M.B. Association. All rights reserved.

Introduction

Malignancies of the oral cavity and oropharynx exhibit aggressive behavior, with a propensity to spread that leads to high attributable mortality rates. Squamous cell carcinoma of the oral and oropharyngeal mucosa is among the six most common cancers (1-3). Risk factors include tobacco use, alcohol consumption (4), human papilloma virus infection (5), male sex, and age of over 55 years (6). This cancer metastasizes to lymph nodes, vertebral fascia, and thorax (7).

In Mexico, squamous cell carcinoma accounts for 90% of oral malignancies. The five-year survival rate is approximately 50% (8). Three treatment modalities are used either alone or in combination for the clinical management of hypopharyngeal cancer: radiotherapy, chemotherapy, and surgery (9). Side effects include nausea, fatigue, mucositis, difficulty in opening the mouth, and dental complications (10).

Metastasis results from interactions between several signaling pathways of oncogenesis, detachment of malignant cells, degradation of extracellular matrices, invasion, migration, adhesion to endothelial cells, angiogenesis, and reinstatement of cells to promote tumorigenesis at distant sites (11). Phosphatidylinositol -3 kinase (AKT-PI-3K) and mitogen-activated protein kinases (MAPK) signaling are upregulated in human squamous cell carcinoma. Activated ERK ½, Notch, WNT/β-catenin, and PI3K/AKT/mTOR pathways have been observed in the FaDu cell line (12).

Moreover, proper oral hygiene and eating habits are very important for the prevention of cancer. Fruit and vegetable consumption has been directly correlated with reduced cancer risk (13-15). Several studies have indicated that nobiletin (NOB), a polymethoxyflavone obtained from the peels of citrus fruits such as mandarins (*Citrus reticulate*), sweet oranges (*Citrus sinesis*), lemons (*Citrus depressa*), and tangarines (*Citrus tangarine*) has beneficial anti-inflammatory, anti-microbial, anti-sclerotic, and anti-tumor activities, and improves memory function (8-10). It is extracted by the supercritical fluid technique used to process freeze-dried peels of citrus fruits. The extracts are then treated with carbon dioxide and ethanol to concentrate bioactive compounds. NOB ($C_{21}H_{22}O_8$) is classified under the flavone family and has a molecular weight of 402.399 g/mol. Its International Union of Pure Applied Chemistry nomenclature is 2-(3,4-dimethoxyphenyl) 5,6,7,8- tetramethoxychromen-4-one; it is also known as 5,6,7,8,3',4'-hexamethoxyflavone or 2-(3,4-dimetoxyphenyl)-4,6,7,9-tetramethoxy-4 H-1-benzopyran-4-one. NOB is metabolized into several derivatives with important anti-cancer effects. NOB reduces cell migration, invasion, and proliferation of renal cell adenocarcinoma cells (12), and also reduces proliferation, induces apoptosis, and inhibits migration of human breast cancer (MCF-7) cells via reductions of matrix metalloproteinase (MMP) 9 expression, p38 activity, and nuclear factor-kB and Nf2 translocation (16-18).

In this study, we examined the effects of NOB on viability, apoptosis, migration, and angiogenesis of a hypopharyngeal squamous cell carcinoma cell line. Our findings suggest that NOB may be a promising candidate for fur-

* Corresponding author. Email: gloriafoodntounam@gmail.com

ther development as an antineoplastic drug.

Materials and Methods

Nobiletin preparation

Nobiletin, 3′,4′,5,6,7,8-Hexamethoxyflavone; 2-(3,4-Dimethoxyphenyl)-5,6,7,8-tetramethoxy-4H-1-benzopyran-4-on (CAS 478-01-3, purity >97%) was dissolved in sterile dimethyl sulfoxide (DMSO) (Sigma, St. Louis Mo, USA) to a 1 x 10^{-2} M concentration.

Cell Culture

FaDu hypopharyngeal squamous-cell carcinoma cells were obtained from the American Type Culture Collection (Manassas, VA, USA). The cells were seeded in Dulbecco's modified Eagle medium (DMEM) (Sigma, St. Louis, MO, USA) supplemented with 10% fetal bovine serum (FBS; Invitrogen, Carlsbad, CA, USA), 1000 µg/mL streptomycin, and 100 µg/mL penicillin (Sigma) in a humidified environment of 5% CO2 in an incubator (Incusafe Sanyo) at 37ºC. Adherent cells were treated with trypsin EDTA (25% v/v) and cultured until adequate confluency was reached, then treated with NOB (Sigma > 97%) from a 10 µM stock solution dissolved in dimethyl sulfoxide (DMSO; Sigma) in amounts ≤1%.

Cytotoxicity Assay

The cells were quantified in a TC20TM automated cell counter (Bio-Rad, Hercules, CA, USA) and seeded at a density of 5 x 104 cells per well for 16 h, then treated with NOB at concentrations of 10, 25, 50, 75, 100, 200, and 300 µM for 24, 48, and 72 h. After each treatment, we removed the medium, added MTT solution (0.5 mg/mL; Sigma) and then incubated the sample for 4 h. The resulting formazan salts were dissolved in acidified isopropanol and measured at 463 nm (Synergy BioTek, Shoreline, WA, USA). We estimated the percentage of live cells relative to that of untreated control cells. The assay was repeated three times in a sextuplicate. We used healthy human gingival fibroblasts as a control.

Wound Healing Assay

10,000 cells were seeded and counted with the TC20TM automated cell counter (Bio-Rad) in a six-well plate and incubated for 16 h, followed by overnight starvation. Wounds were created with a 100-µL micropipette tip. The cells were then incubated in DMEM with 0.5% FBS and treated with 10, 25, 50, 75, and 100 µM NOB at 0 and 24 h. The experiments were conducted three times, with images of 15 locations photographed under a Zeiss Primovert microscope (Carl Zeiss Microscopy, Jena, Germany).

Transwell Migration Assay

We performed a cell migration assay in a Boyden chamber (pore size, 8 µm). We seeded 10,000 cells, counted with a TC20TM automated cell counter (Bio-Rad), into each well of a 24-well plate and suspended them in FBS-free DMEM medium with NOB for the times and at the dosages indicated in Figure 1, for a final volume of 200 µL. We then added 750 µL DMEM medium supplemented with 10% FBS to each well. The cells were fixed with 4% formaldehyde dissolved in phosphate-buffered saline (PBS) for 2 minutes, then washed twice and permeabilized with 100% methanol for 20 minutes. After two washes in PBS, the cells were stained with 0.1 µM thiazole orange (an excitation peak at 514 nm and an emission peak at 533 nm) for 15 minutes, washed twice more with PBS, and cleaned by swabbing. After 4 h, we removed the membranes from the Boyden chamber, observed and imaged them under a Polyvar fluorescence microscope, and analyzed the images using the ImageJ software program (National Institutes of Health, Bethesda, MD, USA). We performed the assay in triplicate, with 25 fields each time.

Gel Zymography

Cells were treated for different time durations with varying NOB dosages. We then collected the culture media. For gel zymography, we measured the protein content using the Bradford method and obtained a final quantity of 50 µg protein. We mixed the protein with Laemmli buffer without 2-mercaptoethanol and incubated the cells at room temperature for 15 minutes. The samples were then loaded onto 8% sodium dodecyl sulfate-polyacrylamide gel electrophoresis (SDS-PAGE) gel with 0.1% gelatin from bovine skin type B (Sigma-Aldrich). After electrophoresis, the gels were washed three times for 20 minutes in zymography buffer [2.5% Triton X100 and 50 mM Tris-HCl (pH 7.5)], and incubated overnight at 37ºC in zymography developer buffer [50 mM Tris-HCl (pH 7.5), 10 mM CaCl2, 5 µM ZnCl2, and 150 mM NaCl]. The gels were then stained with Coomassie Brilliant Blue R-250 (Sigma-Aldrich) for 6 h, followed by destaining for 30 minutes in 7% acetic acid and 40% methanol. The gelatinolytic activity was detected by the presence of clear bands. We performed the experiments three times.

TUNEL Assay

Cells (1 x 105) were grown in 24-well plates on slide covers and treated with NOB (50, 100, 150, 200, and 300 µM) for the times indicated. The slide covers were then processed in the DeadEndTM colorimetric TUNEL system (Promega, CA, USA) according to the manufacturer's specifications. We performed the assays in triplicate, captured different fields by microscopy, and quantified apoptotic bodies.

Western Blot Assay

We examined the expression of apoptosis-associated proteins by western blot analysis. The cells (1 x 106 cells/well) were grown in six-well trays and treated at concentrations indicated in Figures 3-5. After stimulation, we aspirated the medium and detached the cells in a sodium orthovanadate solution in PBS. We performed a western blot assay with a 1:1 mix of 40 µg protein and 2x sample buffer [20% glycerol, 4% SDS, 10% 2-mercaptoethanol, 0.05% bromophenol blue, and 1.25 M Tris-HCl (pH 6.8); Sigma Chemical Co.]. Each sample was loaded on a 7.5% or 10% SDS-PAGE gel and run at 40 V for 2 h. The cell proteins were transferred to a polyvinylidene fluoride membrane (Amersham) for 1 h at 0.3 amps and 15 V. The membrane was then blocked with a skim milk solution for 1 h, washed three times with washing buffer (NaCl, SDS, and Tris base), incubated with primary antibody, and washed again. We used the following antibodies: mouse monoclonal JNK1 antibody (1:1000), mouse monoclonal phospho-JNK (p-JNK) antibody (1:10,000), rabbit polyclonal phospho-PI3K antibody (1:10,000), mouse monoclonal phospho-ERK (p-ERK) antibody (Tyr-204; 1:5000), rabbit

polyclonal ERK 1/2 (1:10,000), mouse monoclonal pp38 antibody (Tyr-182; 1:5000), anti-p38 antibody (1:10,000), mouse monoclonal anti–phospho-AKT antibody (Ser473), phospho-AKT (Thr308; 1:10,000), and goat polyclonal MMP2 and MMP9 antibodies (both 1:10,000; Santa Cruz Biotechnology). In subsequent experiments, the cells were incubated with inhibitors of JNK (20 µM; SP600125), p38 (20 µM; SB203580), MEK (10 µM; PD98059), PI3K (10 µM with 20 nM wortmannin; LY294002) and protein kinase A (PKA, 10 µM) for 24 hours. The membranes were incubated overnight at 4°C, washed three times with washing buffer, and then incubated for 2 h with a secondary antibody (anti-mouse, anti-rabbit, or an-ti-goat immunoglobulin G horseradish peroxidase conjugate, 1:10,000; Santa Cruz Biotechnology). The immunoreactive bands were revealed with a chemiluminescence substrate (Santa Cruz Biotechnology), and an autoradiograph was obtained by exposing the film for 2 min. The samples were analyzed with the LABWORKS laboratory information system.

Enzyme-linked immunosorbent assay (ELISA)

The cells (1 x 106/tray) were grown in six-well trays overnight, then treated with 50 µL NOB and incubated with inhibitors of JNK (20 µM; SP600125), p38 (20 µM; SB203580), MEK (10 µM; PD98059), PI3K (10 µM with 20 nM wortmannin; LY294002) and protein kinase A (PKA, 10 µM) for 24 h. The medium was collected, cell supernatant was centrifuged and 100 µL was used to analyze VEGF expression by enzyme-linked immunosorbent assay, as described by the manufacturer (ENZO Life Sciences, Farmingdale, NY, USA). Assays were performed in triplicate.

RT-PCR Assay

Total RNA was isolated from the FaDu cells treated with NOB (10, 25, 50, 75, and 100 µM) using the Trizol method (Invitrogen), and 1 µg total RNA was then reverse transcribed using the SuperScript IV One-Step RT-PCR system (Invitrogen). We performed RT-PCR using PTEN 5'-AGCTGTGGTGGGTTATGGTCT-3' and 5'-TTTCTAACCGTGCAGGCTCTT-3' (19) and GAPDH 5′-ACCTGACCTCCGTCT AGAAAA-3′ and 5′-ACGCCTGCTTCACCACCTT-3'. Amplification conditions were as follows: denaturation at 94°C for 1 min, alignment at 55°C for 1 min, and extension at 72°C for 1.5 min. PCR was performed for 35 cycles. By electrophoresis with agarose gel (2%) stained with ethidium bromide, we determined the identity of the amplified fragment by its apparent size. We obtained a single band of 285 base pairs for GAPDH. We performed three separate experiments for each treatment.

Assessment of Apoptotic Nuclei

We seeded and grew 1 x 105 cells on slide covers in 24-well plates, then treated them with NOB (25, 50, and 100 µM) for the indicated times. At the end of the treatment, we aspirated the medium and added 250 µL 0.1 µM thiazole orange solution, incubated it for 30 min in the dark, and washed it twice with PBS. We removed the slide covers and placed them on a slide for viewing under a Reichert-Jung Polyvar epifluorescence microscope. We evaluated the role of NOB in apoptosis by analyzing cell morphology. We captured images of 25 random fields at 40X and 100X. The assays were performed in triplicate, and representative images were chosen.

Statistical Analysis

The data are presented as means ± standard deviations for the number of observations. Statistical comparisons were performed with the post-hoc test, the Newman-Keuls test, or the Student's t-test. Differences between means were considered significant at $p < 0.05$.

Results

Effect of NOB on Cell Proliferation

To determine the effect of NOB on cell viability, cells were treated with the following concentrations of NOB: 0, 10, 25, 50, 75,100, 200, and 300 µM, for different periods (24, 48, and 72 h). NOB inhibited proliferation in a time- and dose-dependent manner (Figure 1A) with IC50 61± 0.06, 54.37 ± 0.04, and 31.59 ± 0.03 µM for 24, 48, and 72 h, respectively. Based on the obtained mean inhibitory concentrations (IC_{50} values) (Figure 1A), we selected a dose of 50 µM to evaluate the effects of NOB on FaDu cell migration and invasiveness. Wound healing and Transwell assays disclosed that NOB inhibited wound closure in a dose-dependent manner (Figure 1B) and significantly reduced cell migration at a concentration of 50 µM (Figure 1C), respectively.

Effects of NOB on FaDu Cell Morphology and Apoptosis

TUNEL assay of NOB activity demonstrated dose-dependent apoptotic nucleus formation and changes in cell morphology (Figure 2A) and also revealed dose-dependent formation of apoptotic bodies, with significant differences at a dose of 100 µM (Figure 2B). Western blotting showed that NOB downregulated the Bcl-2/Bax ratio (Figure 2C). These results suggest that NOB reduces cell viability by

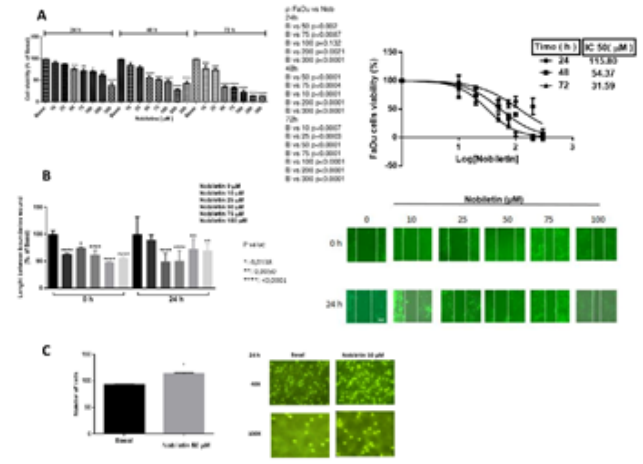

Figure 1. Effect of NOB on wound closure, migration, and invasiveness of FaDu cells. A) Durations and doses of cell treatment with NOB or vehicle (DMSO) on cell viability. B) Mean inhibitory concentration (IC50) for each experimental condition. Experiments were conducted three times in a sextuplicate. B) FaDu cell cultures were subjected to wounding and treated with NOB concentrations of 10, 25, 50, 75 y 100 µM for 24 h. Images of 15 locations were captured under an inverted microscope. The experiments were conducted three times. C) For the migration assay, a Boyden chamber was used for 4 h, in triplicate, with 25 fields each time. *$p < 0.05$, **$p < 0.01$, ****$p < 0.001$ vs. basal.

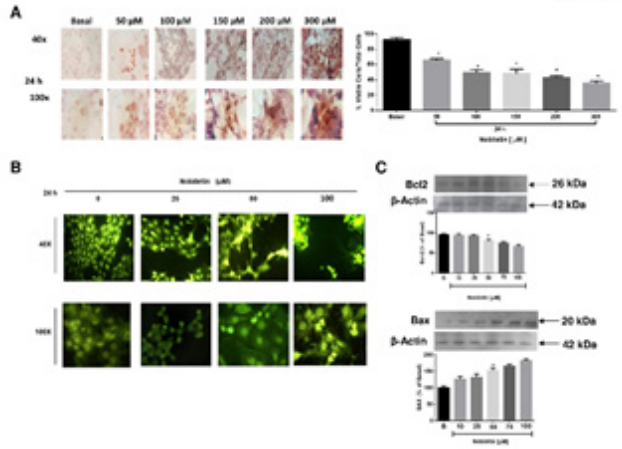

Figure 2. Role of NOB in the induction of apoptosis in FaDu cells. A) FaDu cells were treated with NOB and the TUNEL assay was performed. Images were captured under an optical microscope and apoptotic bodies were quantified. Experiments were performed three times. B) FaDu cells were grown on slide covers to sub-confluency, then treated with NOB and thiazole orange staining. Images were captured under an optical microscope at 40X and 100X. Experiments were performed in triplicate, with imaging of 25 fields each time. C) Apoptosis was evaluated by using western blot analysis to measure pro- and anti-apoptotic protein expressions. Three separate experiments were performed, and data from one were selected as representative. *p < 0.05, **p < 0.01, ****p < 0.001 (ANOVA).

inducing apoptosis.

NOB down-regulated phosphorylation of ERK, JNK, p38, AKT and PI-3K pathways of FaDu cells.

NOB inhibited p-ERK and p-JNK activity (Figure 3A). Additionally, NOB markedly inhibited the PI3K/AKT pathway after 30 min of treatment. We found that NOB inhibited PI3K and phospho-AKT phosphorylation at the threonine 308 and serine 473 sites and upregulated PTEN expression (Figure 3).

NOB Downregulated the Expressions of MMP-2, and MMP-9 F in FaDu Cells

Western blot and RT-PCR analyses showed that NOB downregulated MMP-2 and MMP-9 expressions (Figures 4A and C). In addition, zymography indicated that NOB reduced MMP activity (Figure 4B). These results suggest that NOB inhibits the pro-metastatic properties of FaDu cells.

NOB blocked VEGF expression in FaDu cells.

Additionally, we found that NOB reduced vascular endothelial growth factor (VEGF) levels, suggesting that it may potentially block FaDu cell metastasis and angiogenesis (Figure 5A, 5B). MAPK and PI3K and MEK inhibitors reversed the effects of NOB on viability and VEGF expression in FaDu cells (Figure 5C).

Discussion

Oral squamous cell carcinoma is the most frequently occurring head and neck cancer, with high prevalence and attributable mortality rates among men (17,18, 20). Because its treatment is often complicated by adverse events, the discovery of less toxic therapy is imperative. In this study, we evaluated the effects of NOB on the FaDu cell line, derived from hypopharyngeal squamous cell carcinoma.

Our results showed that NOB induced time- and dose-dependent reductions in cell viability. Similar results were obtained in renal cell carcinoma (21) and breast cancer (22). In nasopharyngeal carcinoma, NOB showed a similar effect as in FaDu cells. NOB inhibited proliferation in oral squamous cell carcinoma (HTB 43) and gliosarcoma (9L) cells at doses of 8 µg/mL (23), and reduced the proliferation of both human pancreatic cancer MIA PaCa-2 and normal ms-1 cells with IC50s of 6.12 µM and 5.5 µM, respectively. We found that NOB reduced FaDu cell prolife-

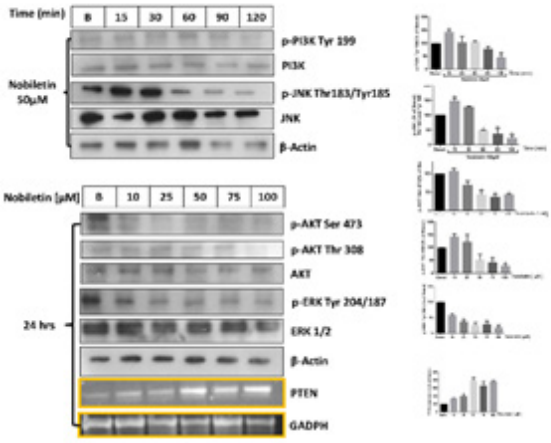

Figure 3. Effect of NOB on the PI3K/AKT and MAPK pathways and PTEN expression. FaDu cells were treated with NOB (10, 25, 50, 75, 100 µM). Total cell lysates were subjected to western blotting with anti-p-PI3 K, p-AKT, p-EKR and p-JNK, and PTEN analysis was used to evaluate PI3K/AKT and MAPK pathway kinases. *p < 0.05, ** p < 0.01, *** p < 0.001 vs. basal (ANOVA).

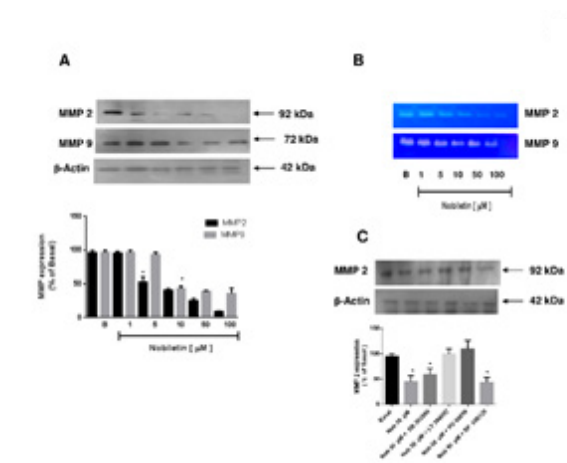

Figure 4. NOB inhibits MMP-2 and MMP-9 protein expression and proteolytic activity. A) FaDu cells were treated with NOB (1, 5, 10, 50 and 100 µM) for 24 h in a free-serum medium and then subjected to western blotting to evaluate protein levels of MMP-2 and MMP9. Protein levels were adjusted with actin. B) FaDu cells were treated with NOB (1, 5, 10, 50, 100 µM) for 24 in free serum medium and then subjected to gelatin zymography to evaluate the activity of MMP-2 and MMP-9. C) Cells were co-treated with NOB (50 µM) and protein kinase inhibitors ERK (PD 98059 20 µM); JNK (SP600125 30 µM); p38 (SB 203580 20 µM) and LY 204002 | µM). * Significantly different p < 0.05 compared with control cells.

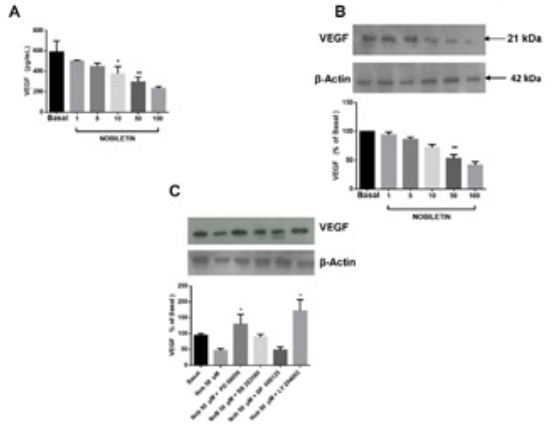

Figure 5. Effect of NOB on VEGF expression. A) Cells were treated with NOB (1, 5, 10, 50, 100 µM) for 24 h in a free-serum medium and then subjected to ELISA analysis. B) Cells were treated with NOB (1, 5, 10, 50, 100 µM) for 24 h in a free serum media and then subjected to western blotting. C) Cells were co-treated with NOB (50 µM) and protein kinase inhibitors of ERK (PD 98059 20 µM); JNK (SP600125 30 µM); p38 (SB 203580 20 µM) and AKT (LY 204002 µM) for 24 h. Experiments were performed three times. *p < 0.05 vs. basal (ANOVA).

ration at higher doses with an IC50 of 115 µM. Moreover, we found that NOB inhibited migration. NOB has been shown to block migration and induce apoptosis of gastric and hepatocellular cells by regulating Bax and Bcl2 expressions (24-26). Similarly, NOB inhibited pancreatic cancer cell migration and invasiveness in wound healing and Transwell assays, respectively, at a dose of 6.12 µM (27), while we found inhibition of FaDu cells at a dose of 50 µM.

NOB (40 µM) induces apoptosis through the intrinsic pathway in ovarian cancer-derived SKOV3/TAX cells (28). We found increased apoptosis at the 50 µM dose. Moreover, we found that NOB inhibits the activation of PI3K/AKT pathway proteins, thereby decreasing the phosphorylation of AKT, PI3K, and mitogen-activated proteins ERK, JNK, p38. We also found that NOB stimulates PTEN expression. This suggests that NOB regulates downstream gene expression in FaDu cells. For this reason, we evaluated the effect of NOB on the expressions of matrix metalloproteinases 2 and 9 and found that NOB downregulated the expressions of these proteins. Similarly, NOB downregulates MMP-2 expression through AKT and MEK. Other studies have shown that NOB inhibits the expression and activity of MMP-2 in nasopharyngeal carcinoma (29). Finally, NOB inhibited the pro-angiogenic factor VEGF through the PI3K/AKT and MEK pathways. Similar results indicate that the AKT pathway regulates VEGF expression in PC-3 and DU-145 prostate cancer cells (30). In conclusion, our results suggest that NOB is a promising drug candidate for the treatment of hypopharyngeal squamous cell carcinoma.

Acknowledgement

To the DGAPA committee for the review and ethical approval of the project IN-230119, August 2, 2019. This research was funded by Dirección General de Asuntos del Personal Académico PAPIIT-230119.

Disclosure statement

There are no conflicts of interest. The authors are alone responsible for the content and writings of the paper.

Authors Contributions

Gloria Gutiérrez-Venegas conceived and designated research, performed tunnel and Transwell assay and wrote the manuscript; Marisol Rosas Martínez performed apoptosis experiment and Western Blots, José Antonio González Rosales performed zymography assays.

References

1. Ferlay J, Colombert M, Soerjomataram I, Mathers C, Parkin DM, Piñeros M, et al. Estimating the global cancer incidente and mortlity in 2018: GLOBOCAN sources and methods. Int J Cancer 2019; 144:1941-1953. https://doi.org/10.1002/ijc.31937
2. Dorak MT, Karpuzuglu E. Gender differences in cancer susceptibility: an indadequately addressed issue. Font Genet 2012; 3:268-279. https://doi.org/10.3389/fgene.2012.00268
3. Pilleron S, Soerjomataram I, Soto-Pérez-de-Celis E, Ferlay J, Vega E, Bray F, et al. Aging and the cancer burden in Latin America and the Caribbean: Time to act. J Geriartr Oncol 2019; 5:799-804. https://doi.org/10.1016/j.jgo.2019.02.014
4. Van der Waal I, de Bree R. Second primary tumours in oral cancer. Oral Oncol 2010; 46(6):426-8. https://doi.org/10.1016/j.oraloncology.2010.02.018
5. Smith EM, Summersgill KF, Allen J, Hoffman HT, McCulloch T, Turek LP, et al. Human papillomavirus and risk of laryngeal cancer. Ann Otol Rhinol Laryngol 2000; 11: 1069-76. https://doi.org/10.1177/000348940010901114
6. Yoo SH, Roh JL, Choi SH, Nam SY, Kim SY. Incidence and risk factors for morbidity and mortality in elderly head and neck cancer patients undergoing major oncological surgery. J Cancer Res Clin Oncol 2016; 6:1343-51. https://doi.org/10.1007/s00432-016-2141-4
7. Nayanar SK, Tripathy JP, Duraisamy K, Babu S. Prognostic efficiency of clinicopathologic scoring to predict cervical lymph node metastasis in oral squamous cell carcinoma. J Oral Maillofac Pathol 2019; 23:36-42. https://doi.org/10.4103/jomfp.JOMFP_132_17
8. Kenneth JV, Jamal MM, Charles LW. Changing pattern of esophageal cancer incidence in New Mexico: a 30-year evaluation. Dig Dis Sci 2010; 55:1622-6. http://doi.org/10.1007/s10620-009-0918-x
9. Lam K, Chan WWL, So TH, Kwong DLW. Systemic Therapy for Esophageal Squamous Cell Carcinoma. Methods. Mol Biol 2020; 2129:321-333. http://doi.org/10.1007/978-1-0716-0377-2_24
10. Chen SB, Huang SJ, Liu DT, Weng HR, Chen YP. Clinicopathological features and prognosis of esophageal squamous cell carcinoma in young patients. Dis Esophagus 2019; 32:1-7. http://doi.org/10.1093/dote/doy070
11. Teófilo CR, Ferreira Junior AEC, Batista AC, Fechini Jamacaru FV, Sousa FB, Lima Mota MR, et al. Mast Cells and Blood Vessels Profile in Oral Carcinogenesis: An Immunohistochemistry Study. Asian Pac J Cancer Prev 2020; 21:1097-1102. http://doi.org/10.31557/APJCP.2020.21.4.1097
12. Albanell J, Codony-Servat J, Rojo F, Del Campo JM, Sauleda S, Anido J, et al. Activated extracellular signal-regulated kinases: association with epidermal growth factor recep-tor/transforming growth factor alpha expression in head and neck squamous carcinoma and inhibition by anti-epidermal growth factor receptor treatments. Cancer Res 2001; 61:6500-10. http://doi.org/11522647
13. Garidou A, Tzonou A, Lipworth L, Signorello LB, Kalapothaki

V, Trichopoulos D. Life-style factors and medical conditions in relation to esophageal cancer by histologic type in a low-risk population. Int J Cancer 1996; 68:295-9. http://doi.org/10.1002/(SICI)1097-0215(19961104)68:3<295::AID-IJC5>3.0.CO;2-X

14. Tzonou A, Lipworth L, Garidou A, Signorello LB, Lagiou P, Hsieh C, et al. Diet and risk of esophageal cancer by histologic type in a low-risk population. Int J Cancer 1996; 68:300-4. http://doi.org/10.1002/(SICI)1097-0215(19961104)68:3<300::AID-IJC6>3.0.CO;2-5
15. Wei D, Zhang G, Zhu Z, Zheng Y, Yan F, Pan C, et al. Nobiletin Inhibits Cell Viability via the SRC/AKT/STAT3/YY1AP1 Pathway in Human Renal Carcinoma Cells. Front Pharmacol 2019; 10:690. http://doi.org/10.3389/fphar.2019.00690
16. Xu Z, Wu D, Fu D, Tang C, Ge J, Zhang Z, et al. Nobiletin inhibits viability of human renal carcinoma cells via the JAK2/STAT3 and PI3K/Akt pathway. Cell Mol Biol (Noisy-le-grand) 2020; 66:199-203. http://doi.org/33040836
17. Saito S, Morishima K, Ui T, Matsubara D, Tamura T, Oguni S, et al. Stromal fibroblasts are predictors of disease-related mortality in esophageal squamous cell carcinoma. Oncol Rep 2014; 32:348-54. http://doi.org/10.3892/or.2014.3216
18. Ogata Y, Hatta W, Koike T, Saito M, Jin X, Nakagawa K, et al. Tohoku Predictors of Early and Late Mortality after Endoscopic Resection for Esophageal Squamous Cell Carcinoma. Tohoku J Exp Med 2021; 253:29-39. http://doi.org/10.1620/tjem.253.29
19. Baek SH, Lee JH, Ko JH, Lee H, Nam D, Lee SG, et al. Ginkgetin Blocks Constitutive STAT3 Activation and Induces Apoptosis through Induction of SHP-1 and PTEN Tyrosine Phosphatases. Phytother Res 2016; 30:567-76. http://doi.org/10.1002/ptr.5557
20. Rao V US, Arakeri G, Subash A, Bagadia RK, Thakur S, Kudpaje AS, et al. Circulating tumour cells in head and neck cancers: Biological insights. J Oral Pathol Med 2020; 49:842-848. http://doi.org/10.1111/jop.13075.
21. Ohnishi H, Asamoto M, Tujimura K, Hokaiwado N, Takahashi S, Ogawa K, et al. Inhibition of cell proliferation by nobiletin, a dietary phytochemical, associated with apoptosis and characteristic gene expression, but lack of effect on early rat hepatocarcinogenesis in vivo. Cancer. Sci 2004; 95:936-42. http://doi.org/10.1111/j.1349-7006.2004.tb03180.x
22. Sp N, Kang DY, Joung YH, Park JH, Kim WS, Lee HK, et al. Nobiletin Inhibits Angiogenesis by Regulating Src/FAK/STAT3-Mediated Signaling through PXN in ER+ Breast Cancer Cells. Int J Mol Sci 2017; 18:935-948. http://doi.org/10.3390/ijms18050935
23. Yang J, Yang Y, Wang L, Jin Q, Pan M. Nobiletin selectively inhibits oral cancer cell growth by promoting apoptosis and DNA damage in vitro. Oral Surg Oral Med Oral Pathol Oral Radiol 2020; 130:419-427. http://doi.org/10.1016/j.oooo.2020.06.020
24. Zheng GD, Hu PJ, Chao YX, Zhou Y, Yang XJ, Chen BZ, et al. Nobiletin induces growth inhibition and apoptosis in human nasopharyngeal carcinoma C666-1 cells through regulating PARP-2/SIRT1/AMPK signaling pathway. Food Sci Nutr 2019; 7:1104-1112. http://doi.org/10.1002/fsn3.953
25. Ma X, Jin S, Zhang Y, Wan L, Zhao Y, Zhou L. Inhibitory effects of nobiletin on hepatocellular carcinoma in vitro and in vivo. Phytother Res 2014; 28:560-7. http://doi.org/10.1002/ptr.5024
26. Wang Y, Wei Z, Pan K, Li J, Chen Q. The function and mechanism of ferroptosis in cancer. Apoptosis. 2020; 25:786-798. http://doi.org/10.1007/s10495-020-01638-w
27. Jiang H, Chen H, Jin C, Mo J, Wang H. Nobiletin flavone inhibits the growth and metastasis of human pancreatic cancer cells via induction of autophagy, G0/G1 cell cycle arrest and inhibition of NF-kB signalling pathway. J BUON 2020; 25:1070-1075.
28. Jiang YP, Guo H, Wang XB. Nobiletin (NOB) suppresses autophagic degradation via over-expressing AKT pathway and enhances apoptosis in multidrug-resistant SKOV3/TAX ovarian cancer cell. Biomed Pharmacother 2018; 103:29-37. http://doi.org/10.1016/j.biopha.2018.03.126
29. Chien SY, Hsieh MJ, Chen CJ, Yang SF, Chen MK. Nobiletin inhibits invasion and migration of human nasopharyngeal carcinoma cell lines by involving ERK1/2 and transcriptional inhibition of MMP-2. Expert Opin Ther Targets 2015; 19:307-20. http://doi.org/10.1517/14728222.2014.992875
30. Chen J, Creed A, Chen AY, Huang H, Li Z, Rankin GO, et al. Nobiletin suppresses cell viability through AKT pathways in PC-3 and DU-145 prostate cancer cells. BMC Pharmacol Toxicol 2014; 15:59. http://doi.org/10.1186/2050-6511-15-59